

## Anisotropic $\gamma$ -ray resonance scattering from a zinc single crystal and the uncertainty principle

R. Moreh and M. Fogel

*Nuclear Research Center-Negev, Beer-Sheva, Israel  
and Ben Gurion University of the Negev, Beer-Sheva, Israel*

(Received 18 April 1994)

The nuclear-resonance photon-scattering technique was used for studying the temperature dependence between 12 and 295 K of the anisotropy in the scattering cross section from the 7362-keV level in  $^{68}\text{Zn}$  using a single crystal of metallic zinc. The anisotropy ratio of the scattering intensities with the beam parallel and perpendicular to the hexagonal planes of Zn was found to increase strongly between 295 and 12 K. This was interpreted in terms of the anisotropic binding of the Zn atoms and was used for deducing the mean-square momenta  $\langle p^2 \rangle_{\perp}$  and  $\langle p^2 \rangle_{\parallel}$  of the Zn atoms at 0 K perpendicular and parallel to the hexagonal planes, and the corresponding Debye temperatures  $\Theta_{\parallel}$  and  $\Theta_{\perp}$ . When these values were combined with the known values of the zero-point vibrational amplitudes  $\langle x^2 \rangle_{\perp}$  and  $\langle x^2 \rangle_{\parallel}$  obtained using the Mössbauer effect, the theoretical lower limit of the uncertainty principle for a metallic solid was found to be reached almost accurately.

### I. INTRODUCTION

In previous publications,<sup>1-8</sup> the nuclear-resonance photon-scattering (NRPS) technique<sup>1,4</sup> was used for studying highly anisotropic systems such as BN which has a hexagonal structure;<sup>5</sup> it was also applied for studying the molecular orientation of anisotropic molecules such as  $\text{HNO}_3$  intercalated in highly oriented pyrolytic graphite<sup>6,7</sup> and of  $\text{N}_2$  adsorbed on Grafoil.<sup>8</sup>

In the present work a nuclear level at 7362 keV in  $^{68}\text{Zn}$  is photoexcited by a chance overlap with a  $\gamma$  line emitted by the  $\text{Cr}(n,\gamma)$  reaction. It has been shown<sup>4</sup> that the scattering cross section  $\sigma_r$  in this particular photoexcitation process is sensitive to the atomic environment of the scattering atom; it was also indicated that  $\sigma_r$  at 300 K changes by a few percent by merely changing the chemical form of the scatterer, e.g., using ZnO or ZnS instead of metallic Zn. These variations in  $\sigma_r$  are strongly enhanced when the temperature of the scatterers was reduced down to 12 K.

Metallic zinc is known to have a hexagonal close-packed structure with a high  $c/a$  ratio of 1.861. Such a high  $c/a$  ratio implies a strong anisotropy whereby the atomic binding between neighboring Zn atoms in the hexagonal planes is stronger than that along the  $c$  axis.

The purpose of the present work is twofold: first to measure the anisotropic binding properties of the Zn atoms in a metallic single crystal by measuring the anisotropy of the resonance photon scattering cross section from the two orientations of the single crystal with respect to the incident photon beam and second to deduce the values of  $\langle p^2 \rangle_{\parallel}$  and  $\langle p^2 \rangle_{\perp}$  which are the zero-point mean-square linear momenta along and perpendicular to the hexagonal planes of the crystal. These were then combined with  $\langle x^2 \rangle_{\parallel}$  and  $\langle x^2 \rangle_{\perp}$  which are the corresponding zero-point mean-square atomic displacements in an attempt to test to what extent the products

$\langle x^2 \rangle_{\parallel} \langle p^2 \rangle_{\parallel}$  and  $\langle x^2 \rangle_{\perp} \langle p^2 \rangle_{\perp}$  conform to the requirements of the uncertainty principle (UP), namely

$$\langle x^2 \rangle_{\parallel} \langle p^2 \rangle_{\parallel} \geq \frac{h^2}{16\pi^2}, \quad (1)$$

$$\langle x^2 \rangle_{\perp} \langle p^2 \rangle_{\perp} \geq \frac{h^2}{16\pi^2}. \quad (2)$$

It is important to point out that the interpretation of the UP which is normally employed refers to a simultaneous determination of both  $\langle x^2 \rangle_{\parallel}$  and  $\langle p^2 \rangle_{\parallel}$  for a single particle while here we specifically deal with an ensemble of particles and with the independent determination of  $\langle x^2 \rangle_{\parallel}$  and of  $\langle p^2 \rangle_{\parallel}$  of the ensemble.

It should be remarked that  $\langle x^2 \rangle_{\parallel}$  and  $\langle x^2 \rangle_{\perp}$  of a single crystal of metallic Zn has already been measured by using the Mössbauer effect in which the 93.3 keV transition in  $^{67}\text{Zn}$  was employed.<sup>9,10</sup> This was done by measuring the anisotropy in the Lamb-Mössbauer factor. In a way the present measurement is therefore complementary to that of the Mössbauer effect whereby a strong atomic binding along the hexagonal planes implies a small  $\langle x^2 \rangle_{\parallel}$  (at  $T=0$  K) and a large  $\langle p^2 \rangle_{\parallel}$ , while weak binding along the  $c$  axis implies large  $\langle x^2 \rangle_{\perp}$  and hence small  $\langle p^2 \rangle_{\perp}$ .

### II. THEORETICAL BACKGROUND

#### A. Effective temperatures

The nuclear-resonance photon-scattering process, studied in the present work is depicted in Fig. 1. It shows the Doppler-broadened shapes of a  $\gamma$  line at  $E_s = 7362$  keV, emitted by the  $\text{Cr}(n,\gamma)$  reaction (represented by a Gaussian<sup>1</sup>) overlapping a resonance level at an energy  $E_r$  in  $^{68}\text{Zn}$  (represented by a  $\psi$  function). The two lines happen to be separated by an energy  $\delta = |E_r - E_s| \approx 20$  eV (after

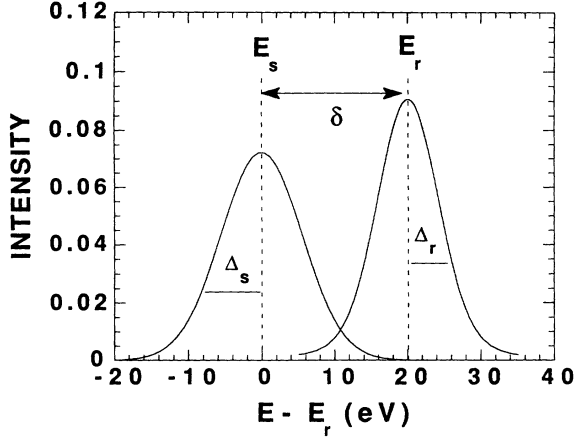


FIG. 1. Calculated shapes of the Doppler-broadened  $\gamma$  line at  $E_s = 7362$  keV [described by a Gaussian (Refs. 1 and 3)] separated by an energy  $\delta = |E_r - E_s| \approx 20$  eV from the resonance level at energy  $E_r$ , (described by a  $\psi$  function). The scattering cross section  $\sigma_r$  is proportional to the overlap integral of the two lines. It is easy to see that  $\sigma_r$  increases with increasing  $\Delta_r$ , and vice versa.

accounting for the recoil energy). The scattering cross section  $\sigma_r$  is proportional to the overlap integral of the two Doppler-broadened shapes. Here, it is tacitly assumed that in the scattering process, the full Doppler broadening of the resonance level is achieved. This situation occurs only when the lifetime of the resonance level ( $\tau \sim 10^{-15}$  s) is much shorter than the time between two collisions ( $\tau \sim 10^{-13}$  s) of the recoiling emitting nucleus. In this case the incident photon is absorbed and remitted long before any “smearing” of the vibrational velocity of the Zn atoms takes place. It should also be noted that because of the large recoil energy in the present case ( $\sim 0.43$  keV), the emitted photon at backward angles is far removed from the resonance condition and hence has no influence on the outgoing channel.

Details of calculating  $\sigma_r$  were published elsewhere.<sup>1,3</sup> Here, we will only mention that  $\sigma_r$  is a function of  $E_r$ ,  $\Delta_s$ ,  $\Delta_r$ ,  $\delta$ ,  $\Gamma_0$ , and  $\Gamma$  where  $E_r$  is the energy of the resonance level;  $\Gamma_0$  and  $\Gamma$  are the ground-state radiative width and the total width of the level.  $\Delta_s$  and  $\Delta_r$  are the Doppler widths of the incident  $\gamma$  line and the nuclear-resonance levels. The Doppler width  $\Delta_r$  of the nuclear level is given by

$$\Delta_r = E_r (2kT_r / mc^2)^{1/2}, \quad (3)$$

where  $m$  is the mass of the scattering isotope and  $k$  is the Boltzmann constant.  $T_r$ , the effective temperature of the scatterer first defined by Lamb<sup>11</sup> to account for the quantum motion of the atomic oscillators, is given by

$$kT_r = \int_0^\infty g(\nu) h\nu \alpha d\nu / \int_0^\infty g(\nu) d\nu, \quad (4)$$

where  $\alpha = [(e^{h\nu/kT} - 1)^{-1} + 0.5]$ .

The phonon density of states  $g(\nu)$  of the scatterer is normalized to unity so that

$$\int_0^\infty g(\nu) d\nu = 1. \quad (5)$$

A similar definition holds for the Doppler width  $\Delta_s$  of the  $\gamma$  line.

The notion of the effective temperature is very important because it gives the total kinetic energy of the atomic oscillator (including that of its zero-point motion). It is thus related to the mean-square zero-point linear momenta of the atoms. Hence, the limiting value of  $T_r$  at 0 K which we denote by  $T_0$  expresses the zero-point kinetic energy of the atomic oscillators and hence is related to the zero-point mean-square linear momenta of the atoms  $\langle p_x^2 \rangle$  (along the photon beam direction) by the relation

$$\langle p_x^2 \rangle = mkT_0. \quad (6)$$

Experimentally, the mean-square zero-point linear momenta of the atoms may be obtained by measuring the photon scattering cross section  $\sigma_r$ , as a function of  $T$  (relative to 295 K) from which the effective temperature  $T_r$  versus  $T$  and hence its limiting value  $T_0$  is deduced.

For anisotropic systems such as a hexagonal single crystal of metallic Zn, we may define two effective temperatures,  $T_{\parallel}$  and  $T_{\perp}$ , in a similar manner to that of Eq. (6) which denotes the limiting values at  $T = 0$  K and are related to the corresponding limiting values  $\langle p^2 \rangle_{\parallel}$  and  $\langle p^2 \rangle_{\perp}$  by

$$\langle p^2 \rangle_{\parallel} = mkT_{\parallel} \quad \text{and} \quad \langle p^2 \rangle_{\perp} = mkT_{\perp}. \quad (7)$$

#### B. Relation to the uncertainty principle

Our purpose is to find to what extent our measured values of  $\langle p^2 \rangle_{\parallel}$  and  $\langle p^2 \rangle_{\perp}$  conform to the requirements of the UP. Obviously, the most interesting point in such a test is to find to what extent one can approach the lowest limit of Eqs. (1) and (2), namely the equality sign. Theoretically, such a situation can only be achieved for a harmonic oscillator (HO) in its ground state. This may be seen by noting that the ground-state wave function  $\phi$  of a HO is a Gaussian, namely

$$\phi(x) = (4\pi m \nu / h)^{1/4} \exp(-2\pi^2 m \nu x^2 / h) \quad (8)$$

and may be used for calculating the quantum-mechanical expectation values of  $\langle x^2 \rangle$  and  $\langle p_x^2 \rangle$  as follows:

$$\langle x^2 \rangle = \int_{-\infty}^{\infty} \phi^* x^2 \phi dx = h / (8\pi^2 m \nu), \quad (9)$$

$$\langle p_x^2 \rangle = \int_{-\infty}^{\infty} \phi^* p_x^2 \phi dx = hm \nu / 2, \quad (10)$$

where the product  $\langle x^2 \rangle \langle p_x^2 \rangle$  is equal to the lowest limit  $h^2 / 16\pi^2$ , with  $\nu$  the frequency of the oscillator. It is important to remind the reader that the above is a very special property of the HO and that a similar calculation using one-dimensional infinite square well potential yields a product  $\langle x^2 \rangle \langle p_x^2 \rangle$  which exceeds the lowest limit of Eq. (1) by 29%. One may also note that for any excited state of the HO, the product  $\langle x^2 \rangle \langle p_x^2 \rangle$  is obviously larger than  $h^2 / 16\pi^2$ .

Experimentally, for a real solid, one can approach the lowest limit of the UP only at very low temperatures where the harmonic approximation is expected to hold and the oscillators are at their ground states. In addition, the physical meaning of  $\langle p_x^2 \rangle$  for a real solid at 0 K is the

mean-square zero-point momenta of the atoms averaged over all the vibrational frequencies of the solid. This is equal to the mean-square uncertainty of the momenta averaged over all atoms of the solid. A similar interpretation applies for the physical meaning of  $\langle x^2 \rangle$ . For a real isotropic solid, these quantities may be obtained by integrating  $\langle x^2 \rangle$  and  $\langle p_x^2 \rangle$  of Eqs. (9) and (10) over the real phonon density of states  $g(\nu)$  yielding

$$\langle x^2 \rangle_s = \frac{h^2}{8\pi^2 m} \int_0^\infty g(\nu) \nu^{-1} d\nu = \frac{h^2}{8\pi^2 m} M_{-1}, \quad (11)$$

$$\langle p_x^2 \rangle_s = \frac{hm}{2} \int_0^\infty g(\nu) \nu d\nu = \frac{hm}{2} M_{+1} \quad (12)$$

with  $M_{-1}$  and  $M_{+1}$  the  $n = -1$  and  $n = +1$  moments of the phonon density of states  $g(\nu)$ . It is of interest to note that  $\langle x^2 \rangle_s$  and  $\langle p_x^2 \rangle_s$  may be identified with the measured  $\langle x^2 \rangle$  and  $\langle p_x^2 \rangle$  for a real solid. In addition,  $M_{-1}$  is in fact identifiable with the Debye-Waller factor.<sup>13</sup> Thus, for a real solid we have

$$\langle x^2 \rangle_s \langle p_x^2 \rangle_s = M_{-1} M_{+1} \left[ \frac{h^2}{16\pi^2} \right]. \quad (13)$$

Obviously, the product  $M_{-1} M_{+1}$  must satisfy the following relation in order to comply with the requirements of the UP, namely

$$M_{-1} M_{+1} \geq 1. \quad (14)$$

Thus for an Einstein solid (where the atoms are assumed to behave as independent HO's having a single frequency) we get the equality sign in Eq. (14), while for a Debye-type phonon density of states  $g(\nu) = 3\nu^2/\nu_d^3$  (where  $\nu_d$  is the Debye cutoff frequency), we get

$$M_{-1} M_{+1} = \frac{9}{8}. \quad (15)$$

Equation (15) means that the lowest limit of the product  $\langle x^2 \rangle_s \langle p_x^2 \rangle_s$  for a Debye solid is larger than that of Eq. (1) by a factor  $\frac{9}{8}$ . For a real solid, we define a factor  $\beta$  which normalizes the product  $M_{-1} M_{+1}$  to that of a Debye solid, namely

$$\beta = (8/9) M_{-1} M_{+1}. \quad (16)$$

Obviously, an experimental value of  $\beta = 1$  or close to it would mean that the measured values of  $\langle p_x^2 \rangle$  conform with the lowest limit of the UP for an isotropic Debye solid.

### III. EXPERIMENTAL METHOD

The experimental system (Fig. 2) consisted of a photon beam, a scattering chamber, a cryostat, and two  $\gamma$  detectors. The photon beam was generated from the  $(n, \gamma)$  reaction on three chromium disks (each 8 cm diam and 1 cm thick) placed near the core of the IRR2 reactor. The resulting photon beam was collimated and neutron filtered using 40 cm of borated paraffin. The intensity of the 7362 keV  $\gamma$  line arising from the  $^{51}\text{Cr}(n, \gamma)$  reaction is  $10^5$  photons/cm<sup>2</sup>s on the scatterer. The target consisted of a cylindrical single crystal of metallic Zn (18 mm diam and 40 mm long) with its  $c$  axis along one radius namely perpendicular to the symmetry axis of the cylinder; it was fitted inside a thin-walled aluminum cylinder and placed in a variable temperature ( $12 \text{ K} \leq T \leq 300 \text{ K}$ ) cryostat. The latter was mounted on a stepping motor which rotated the sample around its symmetry axis from a position in which the photon beam and the  $c$  axis were parallel to a perpendicular position. With such a geometry of the sample, the atomic attenuations of the 7362 keV photons were identical for the two positions of the target with respect to the photon beam. For the high-temperature measurements ( $295 \text{ K} \leq T \leq 523 \text{ K}$ ), a cylindrical polycrystalline metallic Zn disk (75 mm diam, 5 mm thick) placed with its symmetry axis nearly parallel to the photon beam, was used. It was heated after inserting it inside a thin-walled aluminum container and mounting an electrical heater around its circumference. The scattered radiation from the Zn target was detected using two hyper-pure germanium (HPGe) detectors of volumes 150 and 120 cm<sup>3</sup> placed symmetrically at 15 cm and at an angle 120° on both sides of the target. The background radiation spectrum was obtained using a combined metallic target consisting of cobalt and manganese and having identical dimensions and weight to that of Zn. This background was corrected to account for the lower atomic number of Co and Mn with respect to Zn. Other neighboring elements such as Cu and Ga could not be used for simulating the atomic "background" because they were found to be resonant scatterers of some of the lines emitted by the  $\text{Cr}(n, \gamma)$  source. The scattering chamber consisted of thick shielding of lead walls placed around the cryostat and the  $\gamma$  detectors and served to shield the detectors from the external and cosmic background. More details concerning the experimental system were published elsewhere.<sup>12</sup>

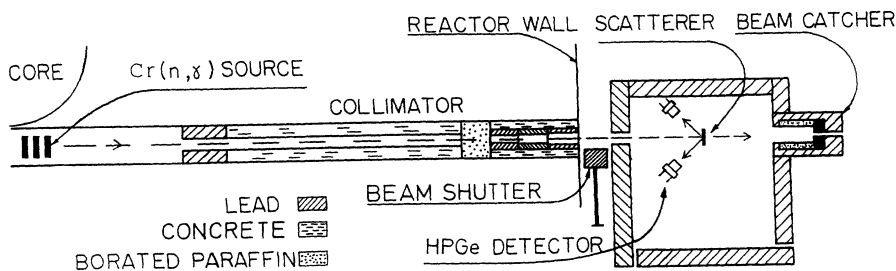


FIG. 2. Schematic diagram (not to scale) of the experimental system showing the chromium  $\gamma$  source, collimator system, sample, surrounding shielding, and the two detectors.

## IV. RESULTS AND DISCUSSION

### A. $T$ dependence of the scattered intensities

Part of the scattered spectra with the photon beam parallel to the  $c$  axis of the Zn crystal is shown in Fig. 3 for a sample temperature of 12 K. The spectrum shows the elastic and only one inelastic component of the scattered radiation from the 7362 keV level in  $^{68}\text{Zn}$ . It was necessary, as explained below, to measure the dependence of the scattered intensity from a polycrystalline metallic Zn on  $T$  in the range 295–523 K in order to determine the value of  $\delta$  (Fig. 1); the results normalized to 295 K are given in Fig. 4. Furthermore, to determine the value of  $T_{\perp}$  we measured the  $T$  dependence of the scattering cross section from a single crystal with the photon beam parallel to the crystal  $c$  axis in the range 294–12 K; the results (normalized to 294 K) are shown in Fig. 5. Note the large drop in the scattered intensity by a factor of about 2 between 294 and 12 K. This is caused by the fact that the energy separation  $\delta$  is very large as will be seen below. To determine  $T_{\perp}$ , it was sufficient to measure the anisotropy  $R = \sigma_{\parallel}/\sigma_{\perp}$  of the scattered radiation from the two geometries of the single crystal with respect to the photon beam at three temperatures 12, 102, and 294 K. The results are given in Table I and plotted in Fig. 6 together with the high-temperature data; it shows the excellent agreement obtained between the measured and calculated values in the 12–523 K temperature range. It should be noted that the high-temperature data of Fig. 6 were in fact taken from Fig. 4 and corrected to account for the different shapes of the targets and different Debye temperatures as explained in Sec. IV E.

### B. Determination of the resonance level parameters

One of the main goals of the present work was to determine the effective temperatures of the Zn crystal,  $T_{\perp}$  and  $T_{\parallel}$ , along the two directions as a function of  $T$  and at 0 K. To do so it is important to have a precise knowledge

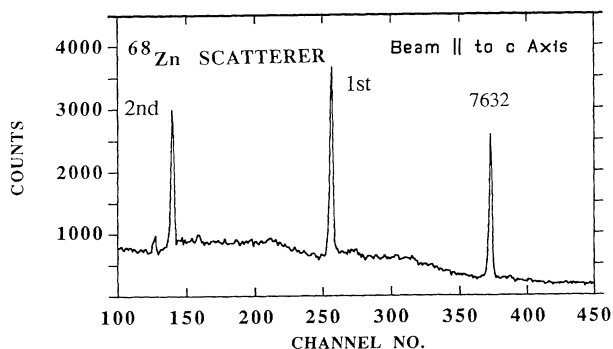


FIG. 3. Portion of the spectrum of the scattered radiation from a single crystal of metallic Zn obtained using a  $150\text{ cm}^3$  HPGe detector with the photon beam parallel to the  $c$  axis. The spectrum was taken at 12 K. The three peaks correspond to the photo, first (1st) and second (2nd) escape peaks of the resonantly scattered 7362-keV  $\gamma$  line. The inelastic peak is visible. The running time was 36 h.

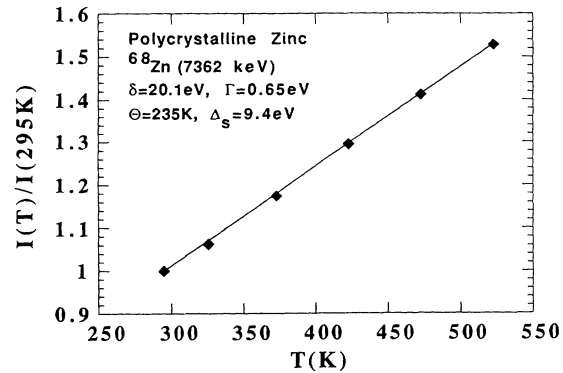


FIG. 4. Measured scattered intensity ratios versus  $T$  in the range 295–523 K from a polycrystalline metallic Zn. The solid line represents the best fitted curve obtained using  $\delta=20.1\text{ eV}$ ,  $\Gamma=0.65\text{ eV}$ ,  $\Gamma_0/\Gamma=0.85$ ,  $\Delta_s=9.4\text{ eV}$ , and  $\Theta=235\text{ K}$ . The dependence on the value of  $\Theta$  is very weak.

of the resonance parameters of the scattering process. The parameters are:  $E_r$ ,  $E_s$ ,  $J$ ,  $T_r$ ,  $T_s$ ,  $\delta$ ,  $\Gamma$ , and  $\Gamma_0$ . They are usually determined by carrying out five independent measurements.<sup>12,14,15</sup> (i) The resonance energy  $E_r$  and the branching ratio  $\Gamma_0/\Gamma$  (where  $\Gamma$  and  $\Gamma_0$  are the total and ground-state radiative widths, respectively) are determined from the resonantly scattered spectrum by comparing the intensities of the elastic and all inelastic lines. In doing so, the intensities were corrected for the detector efficiency (which varies with the energy of the  $\gamma$  lines) and for their atomic attenuation in the shielding material surrounding the detector. (ii) The spin  $J$  of the resonance level is deduced from the angular distribution of the elastically scattered radiation. (iii) The energy separation  $\delta$  (Fig. 1) and  $\Gamma_0$  are found by measuring the vari-

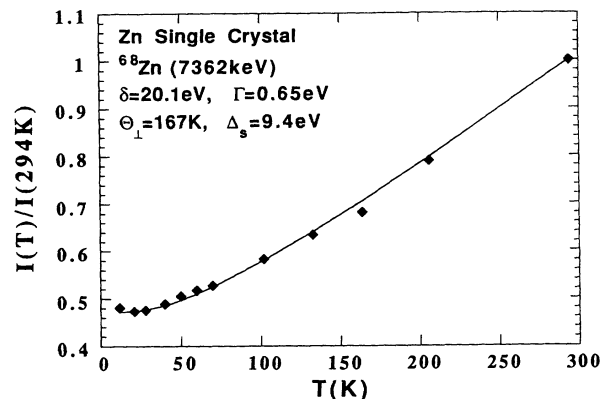


FIG. 5. Measured scattered intensity ratios versus  $T$  in the range 12–294 K from a single crystal of metallic Zn for a case in which the photon beam is perpendicular to the hexagonal planes of the Zn crystal. The effective temperature  $T_{\perp}$  at 0 K was obtained by best fitting the cross-section ratios at the lowest three temperatures 12, 21, and 28 K and extrapolating to 0 K using the following parameters:  $\Gamma=0.65\text{ eV}$ ,  $\Gamma_0/\Gamma=0.85$ ,  $\Delta_s=9.4\text{ eV}$ , and  $\delta=20.1\text{ eV}$ . The solid lines represent the calculated relative cross sections with the same parameters and using  $\Theta_{\perp}=(\frac{8}{3})T_{\perp}=167\text{ K}$ .

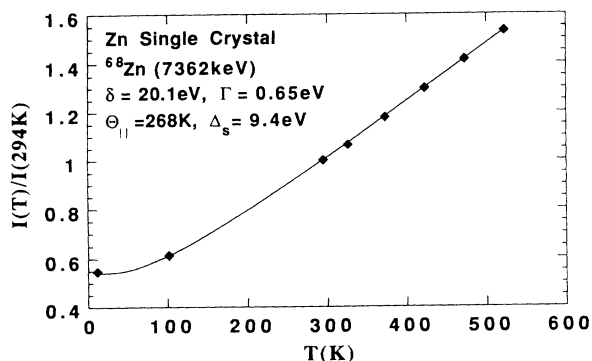


FIG. 6. Measured scattered intensity ratios versus  $T$  in the range 12–523 K from a polycrystalline metallic Zn for a case in which the photon beam is parallel to the hexagonal planes of the Zn crystal. The data above 295 K were deduced from that of a polycrystalline Zn sample (see text). The solid line represents the calculated relative cross sections obtained using the parameters:  $\delta=20.1$  eV,  $\Gamma=0.65$  eV,  $\Gamma_0/\Gamma=0.85$ ,  $\Delta_s=9.4$  eV, and  $\Theta_{\perp}=268$  K.

ation of the scattered intensity with temperature at high  $T$  ( $T \geq \Theta_{\perp}$ , the Debye temperature of the scatterer) and by (iv) a nuclear self-absorption measurement.<sup>12</sup> The  $T$ -variation results are sensitive mainly to  $\delta$  while nuclear self-absorption is sensitive mostly to  $\Gamma_0$ . The consistency of the deduced parameters is checked by (v) measuring the absolute scattering cross section and comparing it to the calculated one.

It should be noted that those parameters were determined in an earlier work<sup>4</sup> using a polycrystalline Zn target. The results were  $E_r=7362$  keV,  $J=1$ ,  $\Gamma_0/\Gamma=0.85 \pm 0.08$ ,  $\delta=26.0 \pm 1.0$  eV,  $\Gamma=1.90 \pm 0.19$  eV. It turned out however that the values of  $\delta$  and  $\Gamma$  as determined in the previous work are incorrect. We reached this conclusion after failing to fit the new high-temperature data and the new single-crystal data using those parameters. This meant that the above parameters were inadequate and it was necessary to find another set consistent with the old and new data. The first three quantities  $E_r$ ,  $J$ ,  $\Gamma_0/\Gamma$  are relatively easy to determine and were used in the present work. Our task was to look for a new pair of values of  $\delta$  and  $\Gamma$  to replace  $\delta=26.0$  eV,  $\Gamma=1.90$  eV (to be called "old parameters") which could satisfy the new and old data. The new parameters are  $\Gamma=0.65 \pm 0.02$  eV and  $\delta=20.1 \pm 0.1$  eV.

In the following we will describe how the new parameters were determined. As a first step we searched for values of  $\delta$  and  $\Gamma$  which satisfied both the high- $T$  data of

TABLE I. Ratios of scattered intensities ( $\sigma_{\parallel}/\sigma_{\perp}$ ), at a few temperatures, from the Zn single crystal with the photon beam parallel and perpendicular to the hexagonal planes of the crystal.

$T$ (K)	$R = \sigma_{\parallel}/\sigma_{\perp}$
12	$1.169 \pm 0.019$
102	$1.066 \pm 0.008$
295	$1.017 \pm 0.004$

Fig. 5 and the self-absorption measurement of a previous work.<sup>4</sup> In the initial search the values of  $T_r$  and  $T_s$  and hence  $\Delta_r$  and  $\Delta_s$  were calculated by assuming some published values of the Debye temperatures<sup>9,14</sup> for Zn and the Cr  $\gamma$  source.

Next, cross-section ratios versus  $\delta$  were calculated and are shown as solid curves in Fig. 7. From such plots it may be seen that the horizontal dashed line corresponding to a measured ratio ( $R=1.530$ ) at 523 K intersects the calculated curve at two values:  $\delta=20.1$  eV and  $\delta=32$  eV. This ambiguity in the value of  $\delta$  could be resolved by considering the results of the self-absorption and the absolute cross-section measurements from which the corresponding value of  $\Gamma$  was also determined. The final values of  $\delta$  and  $\Gamma$  are determined using an iterative procedure. The above ambiguity in  $\delta$  may also be removed by considering the other solutions for  $\delta$  obtained from the intersection of the dashed horizontal line corresponding to the measured ratio ( $R=0.523$ ) at 12 K (see Fig. 7). The two solutions are  $\delta=20.1$  eV and  $\delta=26$  eV. It is thus clear that the correct value is  $\delta=20.1$  eV as it satisfies both the high- $T$  and low- $T$  data. Thus the other values of  $\delta$  should be discarded.

Using those newly determined values of  $\delta$  and  $\Gamma$ , we proceeded to find the limiting value of the effective temperature  $T_{\perp}$  at 0 K from the low- $T$  data of Fig. 5. This was done by fitting the scattering cross-section ratios to the three low-temperature points at  $T=12$ , 21, and 28 K where a saturation effect is observed (Fig. 5). It is very important to emphasize that in this procedure the value of  $T_{\perp}$  and hence of  $\langle p^2 \rangle_{\perp}$  were determined without using the Debye model and hence it is independent of it. In a similar manner we deduced  $T_{\parallel}$  by fitting the measured scattering cross section at 12 K of Table I using the same procedure and employing the same value of  $\delta$  and  $\Gamma$  found above. Using the value of  $T_{\perp}$  found in this manner and employing the Debye model,  $\Theta_{\perp}$  may be deduced using the relation

$$\Theta_{\perp} = \left(\frac{8}{3}\right)T_{\perp} \quad (17)$$

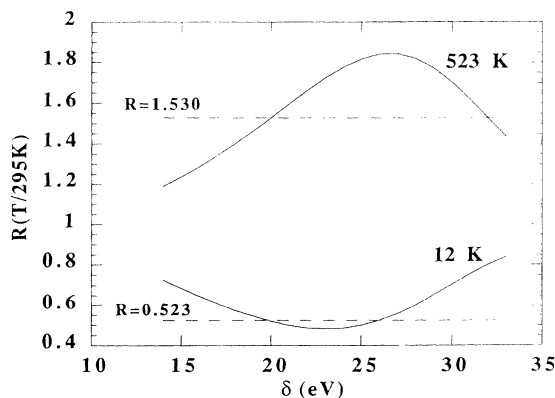


FIG. 7. Calculated scattered intensity ratios at  $T=12$  and 523 K (normalized to 295 K) as a function of the separation energy  $\delta$ . The calculations were made for a 5 mm thick polycrystalline Zn scatterer placed perpendicular to the photon beam with  $\Gamma=0.65$  eV,  $\Gamma_0/\Gamma=0.85$ ,  $\Delta_s=9.4$  eV, and  $\Theta=235$  K. The two horizontal dashed lines correspond to the measured normalized scattered intensity ratios at 12 and 523 K.

which may be obtained from Eq. (5) by calculating the limiting value of  $T$ , when  $T=0$  K by assuming a Debye-type phonon density of states. In a similar manner we deduced  $T_{\parallel}$  by fitting the measured scattering cross-section ratio at 12 K of Table I using the same procedure described above and employing the same value of  $\delta$  and  $\Gamma$ . Here also, the value of the corresponding Debye temperature was determined using the relation  $\Theta_{\parallel}=(\frac{8}{3})T_{\parallel}$ .

The resulting values obtained using the above procedure are  $T_{\perp}=62.6\pm 3.0$  K and  $T_{\parallel}=100.5\pm 4.9$  K which correspond to  $\Theta_{\perp}=167\pm 8$  K and  $\Theta_{\parallel}=268\pm 13$  K. Using these values, the Debye temperature for a polycrystalline Zn is calculated from the relation

$$\Theta_{\perp}=(\Theta_{\perp}+2\Theta_{\parallel})/3=234 \text{ K} . \quad (18)$$

It may be seen that the new values of  $\delta$  and  $\Gamma$  determined in the present work are markedly different from the "old" values. The main reason for the large deviation may be understood by considering Fig. 7 or  $R=0.523$  which allows two solutions for  $\delta$ . In Ref. 4, the second value namely,  $\delta=26.0$  eV was selected from the low-temperature data, as it seemed to agree better with the other experimental measurements. In the present work, however, the new high- $T$  data remove any possible ambiguity as to the correct values of  $\delta$  and  $\Gamma$ . In addition, the results of the self-absorption and the absolute scattering cross-section measurements support the new values of  $\delta$  and  $\Gamma$ .

It is worth noting that despite the uncorrect values of  $\delta$  and  $\Gamma$  used in Ref. 4 the resulting effective temperature at 0 K and the Debye temperature of  $^{68}\text{Zn}$  in polycrystalline Zn, reported in Ref. 4, almost coincides with the present value as determined from  $\Theta_{\perp}$  and  $\Theta_{\parallel}$  in Eq. (18). The reason for this, is very probably due to the fact that the zero-point energies are determined by the saturation behavior of the scattering cross section at low  $T$  and that this value is not very sensitive to the actual values of the parameters  $\delta$  and  $\Gamma$ .

A few remarks concerning the new results are in order. (i) The previous work,<sup>4</sup> contained rather large experimental uncertainties which contributed to the ambiguity in the parameter determination. As an example, the temperature of the Cr  $\gamma$  source in Ref. 4 was estimated but not actually measured, while in the present work, it was monitored and found to be 433 K. (ii) In Ref. 4, the Debye temperature of the Cr  $\gamma$  source was taken as  $\Theta=630$  K instead of the correct value of  $\Theta=473$  K which was obtained recently through a critical study<sup>14,16</sup> using the

NRPS technique on metallic Cr. This fact increased the uncertainty in the resulting values of  $T_{\perp}$  and  $\Delta_{\perp}$ , and hence in the calculated scattering cross section. (iii) In addition, a NaI detector was used in the previous work<sup>4</sup> for measuring the scattered intensities and the net peak areas were deduced by a relatively crude procedure. In the present work however, two large HPGe detectors with excellent resolution were used and the atomic background was subtracted using a combined (Co+Mn) non-resonant scatterers.

### C. Testing the requirements of the uncertainty principle

As mentioned in Sec. II above, the determination of  $T_{\perp}$  and  $T_{\parallel}$  essentially determines the mean-square zero-point linear momenta  $\langle p^2 \rangle_{\perp}$  and  $\langle p^2 \rangle_{\parallel}$  which when combined with those of  $\langle x^2 \rangle_{\perp}$  and  $\langle x^2 \rangle_{\parallel}$  may be used for testing to what extent the corresponding products conform to the requirement of the uncertainty principle. For a Zn single crystal, the values of  $\langle x^2 \rangle$  were determined from a measurement of the Lamb-Mössbauer factor using the 93.3 keV level in  $^{67}\text{Zn}$  by two groups.<sup>9,10</sup> In Table II we used the average of the two reported values and multiplied the result by  $(\frac{67}{68})^{1/2}$  to correct for the different mass between the scattering isotopes in the present work and that of the Mössbauer work. It should also be added that in Ref. 9, two sets of values were reported; in the table we listed only the more recent of the two sets. The calculated products  $\langle x^2 \rangle_{\parallel}\langle p^2 \rangle_{\parallel}$  and  $\langle x^2 \rangle_{\perp}\langle p^2 \rangle_{\perp}$  given in Table II, are expressed in units of  $\frac{9}{8}(h^2/16\pi^2)$  by using the factor  $\beta$  defined in Eq. (16). It may be seen that the results are surprisingly close to unity (namely, to that of a Debye solid) and could just be a coincidence because of the relatively large errors in  $\langle x^2 \rangle$  and the fact that we averaged over two different values of  $\langle x^2 \rangle$ . It should be noted that in a recent paper,<sup>16</sup> some previous studies of the scattering intensities versus  $T$  from other resonance scatterers were analyzed in an attempt to find to what extent the products of the form  $\langle x^2 \rangle\langle p^2 \rangle$  would conform to the requirements of the UP. In this study, the values of  $\langle x^2 \rangle$  were deduced from the phonon density of states  $g(\nu)$  taken from Ref. 13. The result was found to be on the average about 10% higher than that required by the lowest limit of the UP. It was noted, however, that a more accurate test of the above could be done only for a case where an accurate direct determination of  $\langle x^2 \rangle$  is known as is done in the present work for the two directions of the Zn crystal.

TABLE II. Zero-point vibrational amplitudes  $\langle x^2 \rangle_{\parallel}$  and  $\langle x^2 \rangle_{\perp}$  [taken from measurements on  $^{67}\text{Zn}$  using the Mössbauer effect (Refs. 9 and 10)], zero-point energies  $T_{\parallel}$  and  $T_{\perp}$  in K units, and the products  $\langle x^2 \rangle\langle p^2 \rangle$  in units of  $\frac{9}{8}(h^2/16\pi^2)$ , for the two directions of the Zn single crystal. In calculating  $\langle x^2 \rangle\langle p^2 \rangle$ , a correction was applied to  $\langle x^2 \rangle$  to account for the larger mass of  $^{68}\text{Zn}$ .

	$\langle x^2 \rangle$ ( $10^{-3} \text{ \AA}^2$ ) (Ref. 9)	$\langle x^2 \rangle$ ( $10^{-3} \text{ \AA}^2$ ) (Ref. 10)	$T_0$ (K) Present	$\langle x^2 \rangle\langle p^2 \rangle$ $\frac{9}{8}(h^2/16\pi^2)$
Parallel ( $\parallel$ )	$2.03\pm 0.05$	$2.04\pm 0.07$	$100.5\pm 4.9$	$1.004\pm 0.054$
Perpendicular ( $\perp$ )	$3.5\pm 0.05$	$3.0\pm 0.4$	$62.6\pm 3.0$	$0.995\pm 0.108$

The above nice agreement seems to indicate that the harmonic approximation is a very good one at low  $T$  and that values of  $\langle p_x^2 \rangle$  determined by the NRPS are quite accurate as they stand the test of one of the most basic principles of physics. In addition, the Debye model seems to be a very good approximation for the actual properties of metallic solids.

#### D. Testing the phonon density of states of metallic Zn

It is of interest to compare the above findings with the values of  $\beta$  obtained from Eq. (16) using the moments  $M_{-1}$  and  $M_{+1}$  and employing the reported<sup>13,17</sup> phonon density of states  $g(\nu)$  of metallic polycrystalline Zn. In Ref. 13, two phonon spectra are given. The first is an experimental one<sup>17</sup> and the second is calculated theoretically using some Born-von Karman parameters obtained from the force constants of Zn. These two sets of  $g(\nu)$  yield quite different values:  $\beta=1.136$  and  $\beta=1.078$ , respectively. Both  $\beta$  values are much larger than that obtained in the present experiment where it was found to coincide with that of a Debye solid ( $\beta=1$ ) with  $\Theta=234$  K. This result raised the possibility that the large value of  $\beta$  obtained using the phonon spectrum could be related to the fact that Zn has a hcp structure, so we calculated  $\beta$  for other metallic solids having bcc structure (Fe, Cr, Ta) and fcc structure (Al, Ni, Pb) as well as that which have hcp structure (Mg and Tb) using the tabulated density of states of Ref. 13. The results were  $\beta=0.990$ , 0.956, 1.007, 1.016, 0.987, 1.030, 0.979, and 1.00, respectively. This indicates that the values of  $\beta$  for real metallic solids are very close to that of a Debye solid and that the agreement seems to hold to within  $\pm 4\%$ . Here, however, our experimentally deduced  $\beta$  is much lower than the calculated ones obtained from the phonon density of states<sup>17</sup> and more in line with that of other hcp solids. It should however be emphasized that for highly anisotropic layered systems such as pure graphite,<sup>18</sup> a huge deviation from  $\beta=1$  may occur and the result is  $\beta \sim 1.45$ . This behavior may be related to the dimensionality of the solid.

#### E. Comparison with the Debye model

It is very interesting to note that the variation of the scattering cross section with  $T$  for the two perpendicular directions of the single crystal is very nicely described by two Debye temperatures. Figure 5 illustrates this fact for the case where the photon beam is perpendicular to the hexagonal planes of Zn; an excellent agreement may be seen between the measured and calculated curve obtained using a single Debye temperature  $\Theta_{\perp}=167$  K in the range  $12 \text{ K} \leq T \leq 294 \text{ K}$ . A similar situation occurs for the other direction of the Zn single crystal as illustrated in Fig. 7. Here, however, we have plotted the measured cross sections at 12, 102, and 294 K obtained using the Zn crystal together with the high- $T$  data of a polycrystalline Zn which were corrected to account for the difference in sample thickness and Debye temperatures, and for the

fact that the high- $T$  results used  $T=295$  K as a reference temperature. This procedure is justified by the fact that the calculated correction for the above differences between the two targets above 294 K was less than 1%. Here again, excellent agreement between the measured data and the Debye model is obtained using  $\Theta_{\parallel}=268$  K.

Another strong support for the applicability of the Debye model for describing the properties of the Zn single crystal may be found in the compliance of the values of  $\langle x^2 \rangle \langle p_x^2 \rangle$  deduced in the present work with the requirements of the UP as applied to a Debye-type solid. This last result is very significant because the real phonon spectrum of all metallic solids is very different from a Debye spectrum. It seems, however, that the overall effect of the two phonon density of states parallel and perpendicular to the hexagonal planes of the Zn single crystal yield essentially identical results to that obtained from a Debye-type density of states. A similar behavior was found to occur in other polycrystalline solids (e.g., Mg, Al, Cr, Fe, Ni, Tb, Ta, and Pb) as mentioned above. However, in a layered hexagonal system such as graphite, a huge deviation from a three-dimensional Debye behavior was obtained.

#### V. CONCLUSIONS

We have shown that the NRPS technique can be used for the determination of the zero-point linear momenta in a solid scatterer and that the values of  $\langle p_x^2 \rangle$  thus determined conform with the requirements of the UP for a Debye solid to within about 6%. It is very important to emphasize that although we have expressed our measured  $\langle p_x^2 \rangle$  in terms of the Debye temperature, this does not mean that it was necessary to use the Debye model for deducing the values of  $\langle p_x^2 \rangle$  from the measured data. This is because our measured quantities in the present work are the effective temperatures  $T_{\parallel}$  and  $T_{\perp}$  from which the values of  $\langle p^2 \rangle_{\parallel}$  and  $\langle p^2 \rangle_{\perp}$  could be deduced without the need of the Debye temperature or the Debye model. It is nevertheless surprising to see to what extent the measured scattering cross sections versus  $T$  along and perpendicular to the single-crystal  $c$  axis seem to agree nicely with the Debye model. It would be very interesting to carry out more refined measurements of both  $\langle p_x^2 \rangle$  and  $\langle x^2 \rangle$  to find to what accuracy it would be possible to approach the lowest limit of the uncertainty principle. It should be added that a huge deviation from a three-dimensional Debye behavior occurs for a highly anisotropic layered system such as graphite.

#### ACKNOWLEDGMENTS

We would like to thank I. Bergel for technical assistance and help in analyzing the data. I should also like to thank Professor B. Horovitz, Dr. O. Shahal and Dr. Y. Birenbaum for helpful discussions and Dr. W. Potzel from the Technical University of München for useful remarks. This work was supported by the Basic Research Foundation administered by the Israel Academy of Sciences and Humanities.

- <sup>1</sup>R. Moreh, O. Shahal, and V. Volterra, Nucl. Phys. **A262**, 221 (1976).
- <sup>2</sup>O. Shahal and R. Moreh, Phys. Rev. Lett. **44**, 1714 (1978).
- <sup>3</sup>R. Moreh, Nucl. Instrum. Methods **166**, 45 (1979).
- <sup>4</sup>R. Moreh and O. Shahal, Nucl. Phys. **A491**, 45 (1989).
- <sup>5</sup>R. Moreh, Phys. Lett. **41A**, 468 (1985).
- <sup>6</sup>R. Moreh and O. Shahal, Solid State Commun. **43**, 529 (1982).
- <sup>7</sup>R. Moreh, O. Shahal, and G. Kimmel, Phys. Rev. B **33**, 5717 (1986).
- <sup>8</sup>R. Moreh and O. Shahal, Surf. Sci. **177**, L963 (1986).
- <sup>9</sup>W. Potzel, W. Adlassnig, U. Narger, T. Obenhuber, K. Riski, and G. M. Kalvius, Phys. Rev. B **30**, 4980 (1984); W. Potzel, in *Mössbauer Spectroscopy Applied to Magnetism and Materials Science*, edited by G. J. Long and F. Grandjean (Plenum, New York, 1993), Vol. 1, p. 305.
- <sup>10</sup>R. V. Pound, L. Niesen, H. De Waard, and Gui-Lin Zhang, Phys. Rev. B **29**, 6086 (1984).
- <sup>11</sup>W. E. Lamb, Phys. Rev. **55**, 190 (1939).
- <sup>12</sup>R. Moreh, Nucl. Instrum. Methods **166**, 69 (1979).
- <sup>13</sup>H. R. Schober and P. H. Dederichs, in *Photon Dispersion, Frequency Spectra, and Related Properties of Metallic Elements*, edited by K. H. Hellwege, Landolt-Börnstein, New Series, Group III, Vol. 13a (Springer-Verlag, Berlin, Heidelberg, New York, 1981).
- <sup>14</sup>D. Levant, R. Moreh, and O. Shahal, Phys. Rev. B **44**, 386 (1991).
- <sup>15</sup>R. Moreh, O. Shahal, and I. Jacob, Nucl. Phys. **A228**, 77 (1974).
- <sup>16</sup>R. Moreh, in *Capture Gamma-Ray Spectroscopy*, edited by J. Kern (World Scientific, Singapore, 1994), p. 962; R. Moreh, Phys. Lett. B **331**, 13 (1994).
- <sup>17</sup>I. P. Ereemeev, I. P. Sadikov, and A. A. Chernysov, Sov. Phys. Solid State **18**, 960 (1976).
- <sup>18</sup>R. Nicklow, N. Wakabayashi, and H. G. Smith, Phys. Rev. B **5**, 4951 (1972).